ARL-TR-8800 ● SEP 2019

DEVCOM ARMY RESEARCH LABORATORY

Fabrication of High-Strength Lightweight Metals for Armor Applications

by Vladimir M Segal, Phillip J Young, Laszlo J Kecskes, and Vincent H Hammond

NOTICES

Disclaimers

The findings in this report are not to be construed as an official Department of the Army position unless so designated by other authorized documents.

Citation of manufacturer's or trade names does not constitute an official endorsement or approval of the use thereof.

Destroy this report when it is no longer needed. Do not return it to the originator.

ARL-TR-8800 ● SEP 2019

Fabrication of High-Strength Lightweight Metals for Armor Applications

Vladimir M Segal and Phillip J Young
Engineered Performance Materials

Laszlo J Kecskes (Ret.) and Vincent H Hammond
Weapons and Materials Research Directorate, CCDC Army Research Laboratory

REPORT DOCUMENTATION PAGE

Form Approved
OMB No. 0704-0188

1. REPORT DATE *(DD-MM-YYYY)*	2. REPORT TYPE	3. DATES COVERED (From - To)
September 2019	Technical Report	1 August 2016–28 February 2019

4. TITLE AND SUBTITLE
Fabrication of High-Strength Lightweight Metals for Armor Applications

5a. CONTRACT NUMBER

5b. GRANT NUMBER

5c. PROGRAM ELEMENT NUMBER

6. AUTHOR(S)
Vladimir M Segal, Phillip J Young, Laszlo J Kecskes,* and Vincent H Hammond

5d. PROJECT NUMBER

5e. TASK NUMBER

5f. WORK UNIT NUMBER

7. PERFORMING ORGANIZATION NAME(S) AND ADDRESS(ES)
CCDC Army Research Laboratory†
ATTN: FCDD-RLW-MF
Aberdeen Proving Ground, MD 21005

8. PERFORMING ORGANIZATION REPORT NUMBER
ARL-TR-8800

9. SPONSORING/MONITORING AGENCY NAME(S) AND ADDRESS(ES)

10. SPONSOR/MONITOR'S ACRONYM(S)

11. SPONSOR/MONITOR'S REPORT NUMBER(S)

12. DISTRIBUTION/AVAILABILITY STATEMENT
Approved for public release; distribution is unlimited.

13. SUPPLEMENTARY NOTES
* Laszlo J Kecskes was with ARL when the project began. He is now retired from the federal government and is now an assistant research professor at the Hopkins Extreme Materials Institute at Johns Hopkins University.
† The work outlined in this report was performed while the US Army Research Laboratory (ARL) was part of the US Army Research, Development, and Engineering Command (RDECOM). As of 1 February 2019, the organization is part of the US Army Combat Capabilities Development Command (formerly RDECOM) and is now called CCDC Army Research Laboratory.

14. ABSTRACT

This report describes the post-construction modification of the large-scale tooling necessary for the equal channel angular extrusion (ECAE) processing of lightweight structural alloys of AA5083 and AZ31. The "semicontinuous" (sc) ECAE process was successfully demonstrated at a 60- × 60- × 10-cm scale for both alloy systems. However, subsequent conventional rolling operations could not be completed due to failure of the as-rolled billets by "alligatoring". Instead, a roll-forging process was developed to roll the as sc-ECAE processed billets to a 1-inch final thickness.

The evolution of the microstructure and properties was also analyzed for the AA5083 and AZ31 alloys, as model materials representing, respectively, the structural refinement under severe plastic deformation by strain-induced formation of sub-grain boundaries and by dynamic recrystallization. For AA5083, the microstructure after sc-ECAE is composed of ultrafine sub-grains that were further transformed into sub-micrometer grains during subsequent rolling. The preliminary solution treatment of AA5083 was found to be an important stabilizing factor in achieving high mechanical properties. For the AZ31 alloy, optimized sc-ECAE resulted in remarkable structural refinement and well-balanced properties with a low number of passes. However, additional rolling in this case led to a degradation of the structure and properties. In the latter part of the project, the key components for transitioning the sc-ECAE process into a semi- to fully automated forging press manufacturing line were identified and their pertinent aspects described.

15. SUBJECT TERMS
severe plastic deformation, equal channel angular extrusion, structure evolution, grain refinement, mechanical properties, automation, manufacturing transition

16. SECURITY CLASSIFICATION OF:			17. LIMITATION OF ABSTRACT	18. NUMBER OF PAGES	19a. NAME OF RESPONSIBLE PERSON
a. REPORT	b. ABSTRACT	c. THIS PAGE			Vincent Hammond
Unclassified	Unclassified	Unclassified	UU	54	19b. TELEPHONE NUMBER (Include area code) 410-278-2752

Contents

List of Figures v

List of Tables vii

1. Introduction 1

2. The Effects of Combined Semicontinuous ECAE Processing and Rolling on AA5083 and AZ31 Alloys Using Small-Scale Billets 3

2.1 Semicontinuous Multipass ECAE 3

2.2 Optimization of Semicontinuous ECAE of AA5083 4

2.2.1 Material Conditions 4

2.2.2 Microstructures of the Original Materials 5

2.2.3 Structures after 4(D) ECAE Passes 7

2.2.4 Rolling of sc-ECAE-Processed AA5083 10

2.2.5 Mechanical Properties 14

2.3 Optimization of Semicontinuous ECAE of Magnesium Alloy AZ31 16

2.3.1 Microstructure Refinement 16

2.3.2 Rolling of sc-ECAE-Processed AZ31 Material 20

2.3.3 Mechanical Properties of AZ31 22

3. Large-Scale ECAE Tooling and Processing Approach 23

3.1 Tooling Die Modifications 23

3.2 Tooling Die Heating System Modifications 23

3.2.1 Development of the Die Heating System 23

3.2.2 Testing the Die Heating System 25

3.2.3 ECAE Processing Modifications 26

3.3 Large-Scale ECAE Processing of AA5083 Billets 27

3.4 Rolling of ECAE-Processed Billets: AA5083 27

3.5 Large-Scale ECAE Processing of AZ31 Billets 30

3.6 Rolling of the ECAE-Processed AZ31 Billets 30

4. Automation Concept for Large-Scale ECAE Operations 31

4.1 Introduction 31
4.2 An Analysis of Large-Scale ECAE at ETF 32
4.2.1 Layout of the Processing Area 32
4.2.2 Breakdown and Analysis of the Operations 33
4.3 The ECAE Automation Line 34
4.3.1 General Concepts 34
4.3.2 Material Flow 35
4.3.3 Preheating Oven 35
4.3.4 Billet Transferring Conveyors 36
4.3.5 Robots 37
4.3.6 Billet/Tool Lubrication 38
4.3.7 Control System 38
4.3.8 Technical Characteristics and Economic Factors 39

5. Conclusions 39

6. Suggestions for Future Work 41

7. References 43

List of Symbols, Abbreviations, and Acronyms 44

Distribution List 45

List of Figures

Fig. 1 Optical microstructure of the as-received material 5

Fig. 2 EBSD color-coded orientation map of the solution-treated material.... 6

Fig. 3 Optical microstructure of the overaged material 6

Fig. 4 Distribution of the particles in the original as-received material..... 7

Fig. 5 Optical microstructure of the as-received material after 4(D) sc-ECAE passes at 250 °C 8

Fig. 6 Optical microstructure of the solution-treated material after 4(D) sc-ECAE passes at 250 °C..... 8

Fig. 7 Optical microstructure of the overaged material after 4(D) sc-ECAE passes at 250 °C..... 8

Fig. 8 EBSD analysis of the as-received material after sc-ECAE: a) image quality map (step size is 70 nm); b) color-coded orientation map; and c) misorientation angle histogram (5° is set as the minimum) 9

Fig. 9 Edge cracks after reduction of 93.75%: a) as-received material; b) as-received material + 4(D) sc-ECAE passes; c) solution-treated material + 4(D) sc-ECAE passes; and d) overaged material + 4(D) sc-ECAE passes 10

Fig. 10 Optical microstructures of the solution-treated material after rolling reductions of 50% in a), 75% in b), and 87.25% in c)..... 11

Fig. 11 Overview of mid-thickness segregation in the billet in (a, ×10), and intermetallic particle concentrations in the center (b, ×1000) and the off-center (c, ×1000) areas..... 12

Fig. 12 EBSD analyses of the as-received material after sc-ECAE + 50% rolling reduction: a) image quality map (step size is 25 nm); b) color-coded orientation map; and c) misorientation angle histogram (5° is set as the minimum) 13

Fig. 13 Effect of rolling reduction on hardness: 1) as-received material; 2) as-received + overaged + 4(D) sc-ECAE passes; 3) as-received material + 4(D) sc-ECAE passes; and 4) as-received material + solution treated + 4(D) sc-ECAE passes..... 14

Fig. 14 Effect of rolling reduction on YS, UTS, and EL: 1) YS of the solution-treated condition; 2) UTS of the solution-treated condition; 3) EL of the solution-treated condition; and 4) UTS of discontinuous ECAE of the as-received material 15

Fig. 15 Representative microstructure of the original as-received AZ31 material 18

Fig. 16 Microstructure of AZ31 after one pass at 225 °C..... 18

Fig. 17 Microstructure of AZ31 after one pass at 250 °C..... 18

Fig. 18 Microstructure of AZ31 after one pass at 275 °C. Note the considerable larger grains compared to those at lower extrusion temperatures. 19
Fig. 19 Microstructure of AZ31 after two passes at 250 °C 19
Fig. 20 Microstructure of AZ31 after two passes at 275 °C 20
Fig. 21 Microstructure of AZ31 after two passes at 300 °C 20
Fig. 22 Microstructure of the original AZ31 after 50% rolling reduction at 300 °C 21
Fig. 23 Microstructure of the original AZ31 after 87.5% rolling reduction at 300 °C 21
Fig. 24 Microstructure of AZ31 after 2(B) passes of sc-ECAE at 275 °C + 50% rolling reduction at 300 °C 21
Fig. 25 Microstructure of AZ31 after 2(B) passes sc-ECAE at 275 °C + 87.5% rolling reduction at 300 °C 22
Fig. 26 The redesigned tool with the new DHS (without the covers in place; the thermal insulation and tops and electrical connections to the heater cartridges can be seen) 24
Fig. 27 Testing the DHS 24
Fig. 28 Fully assembled large-scale ECAE die with the DHS at the 11,000-ton Ellwood press 25
Fig. 29 ECAE-processed AA5083 billet 27
Fig. 30 Alligatoring of a full-scale large billet of AA5083 during rolling 29
Fig. 31 Alligatoring of sample 2 29
Fig. 32 Alligatoring of sample 3 29
Fig. 33 Rolling of sample 1 30
Fig. 34 Fracture of AZ31 after rolling 31
Fig. 35 Floor plan of the processing area at ETF 32
Fig. 36 Billet-handling operations at ETF 33
Fig. 37 Concept of the ECAE automation line mounted at the forging press 34
Fig. 38 Top-down view of the ECAE automation line 35
Fig. 39 Preheating oven 36
Fig. 40 Conveyors and nesting table 37
Fig. 41 Robot 37
Fig. 42 Billet lubrication chamber 38
Fig. 43 Channel lubrication robot 38

List of Tables

Table 1 Hardness HRB of the AA5083 materials 7

Table 2 Mechanical properties of AA5083 after various processing routes 16

Table 3 Tensile properties of AZ31 in different conditions 22

Table 4 Testing protocols and data for the DHS at the 11,000-ton Ellwood press 26

Table 5 Maximum press load during four passes ECAE of AA5083 27

Table 6 Description and characterization of the ECAE operations 33

Table 7 Calculated characteristics of the oven 36

1. Introduction

The well-known Hall–Petch equation describes the ability to increase the strength of metallic materials by reducing the grain size. Historically, the methods used to achieve the desired grain size reduction in a metal—such as rolling, forging, or extrusion—also resulted in an appreciable dimensional change (e.g., from large diameter to small diameter) in the final piece relative to the starting material. Thus, the amount of deformation and grain size refinement that could be achieved in the material was limited by these dimensional changes.

However, the invention and continued development of equal channel angular extrusion (ECAE) have provided the materials science community with a processing method for imparting a nearly unlimited amount of deformation and hence grain refinement in a metallic work piece. As the name implies, the work piece is extruded around an angle in which the pathway or channel before and after the angle is of the same dimensions. Thus, after a minimal amount of preparation prior to each pass, the work piece can be repeatedly extruded until the desired strain level is achieved. Moreover, the work piece can also be rotated between passes, thereby changing the manner in which the deformation is imparted and the microstructure is refined during the pass.

The potential of the ECAE process to achieve a large degree of microstructural refinement and concomitant strength increases, making it an obvious selection when the US Army Research Laboratory (ARL) was evaluating various severe plastic deformation processing methods for producing ultrahigh-strength metallic alloys in plate form. A 5-year effort focused on AZ31 magnesium alloys that resulted in material with an ultimate strength of 425 MPa, a value approximately 40% higher than that typically reported for the alloy. A key aspect of this effort was the development of ECAE routes that involved temperature step-downs during the multipass processing routine. Such step-downs helped to suppress twinning and shear localization as well as reduce anisotropy by minimizing texture in the alloy plate. However, laboratory-scale equipment restrictions limited developmental efforts to plates no larger than 15.24 × 15.24 × 1.27 cm.

In recognition of this limitation, a Phase I Small Business Innovative Research (SBIR) project was awarded to Engineered Performance Materials LLC (EPM—Whitmore Lake, Michigan) to transition the ECAE processing methodology from the laboratory to the industrial scale. During this effort, a series of modifications were made to the tooling and method such that an AA5083 plate on the order of 38.6 × 38.1 × 8.13 cm^3 could be successfully processed at 250 °C for four passes. These plates were then rolled to a final thickness of 2.5 cm prior to a series of

physical and mechanical testing. Both the ECAE and the ECAE+Rolled plates showed significant strength improvements relative to an annealed or hardened AA5083 plate. A more detailed report of this effort can be found in ARL-TR-6815.[1]

Based upon the success of the Phase I effort, a Phase II SBIR award was made to EPM in late 2012, with work beginning in early 2013. In this subsequent effort, the maximum billet size was further increased to approximately 60 × 60 × 10 cm^3. In addition, a new extrusion concept and several key tooling modifications were developed that resulted in the extruded billet being rectangular in shape with uniform thickness and free from flash or other macroscale defects. This is a significant accomplishment as it further transitions ECAE from a very "hands-on" approach with time-consuming billet modification steps between passes to a process that is more semicontinuous and industrially relevant. Industrial trials performed on AA5083 billets conducted in November 2015 and February 2016 demonstrated that all die systems—such as billet insertion, extrusion, ejection, and trimming—worked as designed for all trials. However, the inability to fully maintain the desired process temperature profiles for both the billet and the die assembly prevented the successful processing of the billets up to four passes. In addition, it was recognized that new approaches were needed to minimize the delay between passes, as this also resulted in an undesired temperature reduction in the billet. Complete details are available in ARL-TR-8047.[2] Due to the cost of retrofitting the tooling, it was deemed necessary that another Phase II SBIR was necessary to prove out the upscaling concept.

Thus, in an effort to further develop ECAE into an industrially applicable process, EPM was awarded a two-year Phase II–Continuation SBIR Project in 2016. Due to limited access to the 11,000-ton forging press (Ellwood Texas Forge [ETF], Houston, Texas) needed to perform the extrusions, the project was extended to February 2019. Based on the efforts of the previous Phase II SBIR project, and in accordance with the original EPM proposal, the project included the following objectives:

1) Determine the effect of combined semicontinuous ECAE processing and rolling on aluminum alloy (AA) 5083 and magnesium alloy AZ31 using small-scale billets.

2) Design, fabricate, and operationally demonstrate an automated die heating system (DHS) for the large-scale ECAE die.

3) Complete modification to the die and auxiliary equipment at the ETF press facility.

4) Complete adjustments to the large-scale ECAE processing sequence.

5) Process large-scale ECAE billets of AA5083 and AZ31 and subsequently roll to 2.5-cm-thick plates.

6) Develop the conceptual design of an automated industrial line for ECAE processing of large-scale billets.

2. The Effects of Combined Semicontinuous ECAE Processing and Rolling on AA5083 and AZ31 Alloys Using Small-Scale Billets

2.1 Semicontinuous Multipass ECAE

Typically, ECAE processing of aluminum and magnesium alloys requires six to eight passes at temperatures of 100–300 °C. In all known cases, this process is performed stepwise—that is, discontinuously, in which the attainment of the required number of passes comprises a sequence of separate steps of billet heating, extrusion in the ECAE die, ejection from the die, cooling in air or water, cleaning/reshaping, and reheating for the following pass. For obvious reasons, such a processing sequence is low production and expensive. The specialized tooling invented and developed by EPM and implemented at a large scale during Phase II of this project enables, for the first time, the semicontinuous, multistep, large-scale ECAE "pass-by-pass" processing without the need for billet cooling, reshaping, and reheating. This innovation significantly increases productivity and transforms ECAE in cost-effective industrial operations that potentially can be performed on fully automated lines.

It must be realized that many aspects of semicontinuous ECAE (sc-ECAE) processing are different in comparison with published results and recommendations on the structure-properties relationships established for discontinuous multipass ECAE. For example, at the typical temperatures for warm discontinuous ECAE operations, time and temperature during processing as well as during recovery can lead to significant structural evolution in the material. In contrast, during sc-ECAE operations, the elapsed time for material handling between passes is only 10–30 s instead of tens of minutes or hours during discontinuous ECAE. Therefore, in the latter case, the structural evolution during multipass ECAE approximates to one-step processing with incremental strain accumulation. While this may seem limiting, due to the adiabatic heating, the actual processing temperature is substantially higher for sc-ECAE, and thus it may exceed the recrystallization temperature of the material. As such, the existence of these different conditions illustrates the availability of additional options to control structure but, at the same time, they may induce certain

complications. Therefore, sc-ECAE must be carefully applied to each new material type to identify the appropriate processing conditions.

2.2 Optimization of Semicontinuous ECAE of AA5083

2.2.1 Material Conditions

AA5083 is a non-heat-treatable aluminum alloy hardened by straining. The main alloying elements are Mg and Mn with lesser additions of Si, Fe, Cu, Zn, Cr, and Ti. Such multicomponent systems produce numerous intermetallic compounds in the form of constituent particles (Al + Fe, Mn, Si with a size range of 0.5–10 μm), dispersions (Al + Mg, Mn, Cr, Zn with a size range of 0.05–0.5 μm), and precipitates (beta phase Mg_2Al_3 of a nanometer size). The constituent particles observed by optical microscopy are formed during solidification and cannot be modified by heat treatment or subsequent thermomechanical processing. The dispersions, formed during homogenization, usually are also not controllable, as their re-solution requires high temperatures and leads to grain growth. Control of nucleation and growth of the Mg-rich precipitates in the Al solid solution (alpha phase) needs long-term annealing cycles at sufficiently low temperatures. Generally, these precipitates do not improve the material strength but affect other characteristics, such as stress corrosion, ductility, mechanical properties at cryogenic temperatures, electrical conductivity, etc.

The implementation of sc-ECAE presents new opportunities to modify the characteristics of the dispersions and precipitates. Because of the dramatic structural refinement and severe straining achieved in short times at low temperature, the partial re-solution of second phases that occurs in the ECAE process does not result in material property degradation due to grain growth. When combined with dynamic strain aging and dynamic recrystallization, this approach provides the potential for optimizing the size and density of dispersions and precipitates.

To investigate and explore these opportunities, a set of special experiments were performed for three AA5083 treatment conditions:

- As-received rolled plate material with H321 temper conditions comprising casting, homogenization, hot and cold rolling, and low-temperature recovery annealing;
- As-received and solution-treated material comprising heating to 530 °C, soaking at temperature for 1.5 h, followed by a water quench; and

- As-received overaged material comprising heating to 530 °C, soaking at temperature for 1.5 h, and slowly cooling in a furnace to room temperature.

Experiments on sc-ECAE with four passes, via Route D (i.e., 90° rotation after each pass), were performed on 15 × 15 × 3.125 cm^3 plate billets using the EPM prototype die and a hydraulic press with a capacity of 450 ton. Billets for all three conditions were heated to 250 °C. The die was preheated to 200 °C. Results of the material characterization are presented in the following sections.

2.2.2 Microstructures of the Original Materials

Microstructures for the three conditions are shown in Figs. 1–3. The as-received and recovery-annealed material (Fig. 1) has a typical heavy-rolled structure that consists of strongly elongated grains of an average grain size (40–50 μm) with many different-size particles. For the solution condition (Fig. 2), etching the polished samples was complicated because of the full dissolution of precipitates, and the microstructure could only be unveiled by the electron backscatter diffraction (EBSD) technique. The microstructure for the overaged condition (Fig. 3) was observed by optical microscopy. In the latter two cases, high-temperature heat treatment results in coarse microstructures that have formed mostly by the growth of large grains (up to a few millimeters in size) during secondary recrystallization.

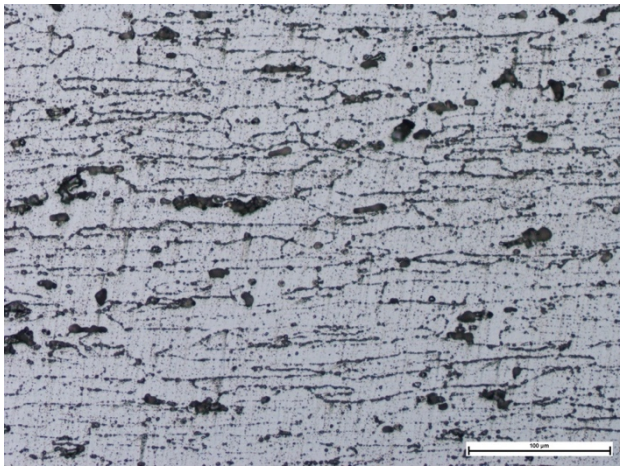

Fig. 1 Optical microstructure of the as-received material

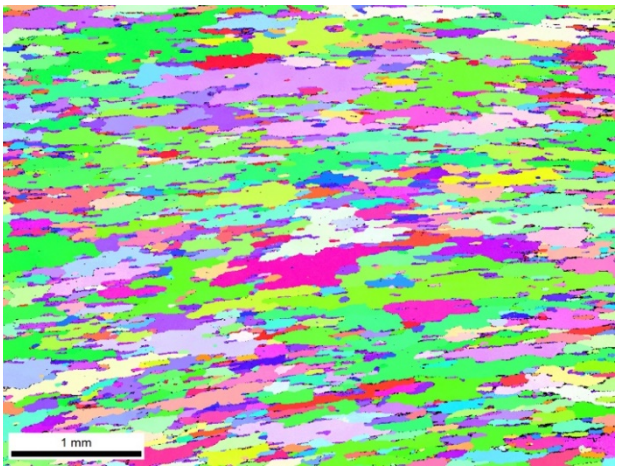

Fig. 2 EBSD color-coded orientation map of the solution-treated material

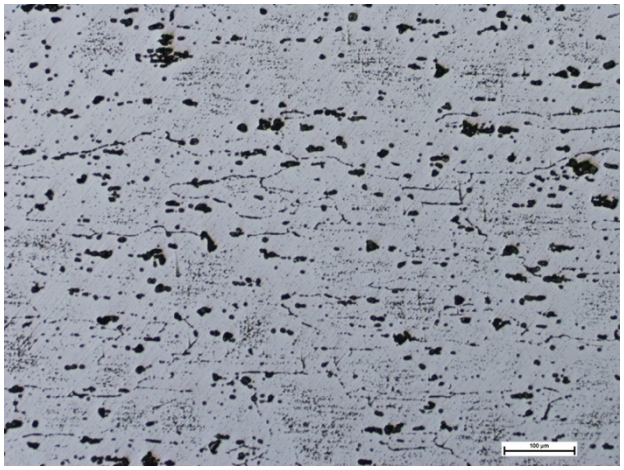

Fig. 3 Optical microstructure of the overaged material

The distribution of particles detected by scanning electron microscopy (SEM) in all cases were identical (Fig. 4). These data correlate with the material hardness (Rockwell B) for the three original conditions measured immediately after heat treatment and 10 days after the heat treatment (Table 1). Note that the solution condition demonstrates a small amount of natural ageing, whereas the as-received and overaged conditions are stable.

Fig. 4 Distribution of the particles in the original as-received material

Table 1 Hardness HRB of the AA5083 materials

Material condition	As-received	Solution-treated	Overaged
Original hardness	32.2	24.2	22.2
After 10 days at room temperature	32.2	26.2	22.2
After 4(D) passes ECAE at 250 °C	47.5	53.8	44.5

2.2.3 Structures after 4(D) ECAE Passes

Table 1 includes the hardness data (Rockwell B hardness HRB), after sc-ECAE for the as-received, solution-treated, and overaged conditions. The highest value was observed for the solution-treated condition due to the additional precipitation hardening during warm ECAE. Figures 5–7 show optical micrographs after sc-ECAE for all material conditions. In all cases, individual and separated grains could not be visualized at magnifications less than 1000×, thereby confirming significant grain refinement. The as-received condition preserves the laminated microstructure of the original material induced by cold rolling as well as the oriented distribution of large particles along the rolling direction similar to that shown in Fig. 4. In contrast, microstructures of the fully recrystallized solution-treated and overaged conditions are isotropic with a more uniform distribution of large particles.

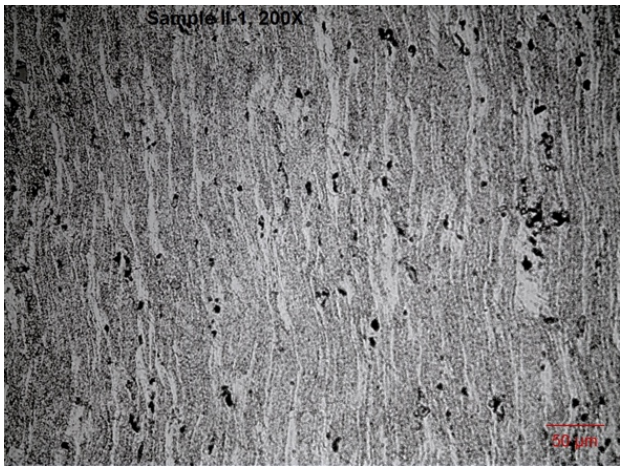

Fig. 5 Optical microstructure of the as-received material after 4(D) sc-ECAE passes at 250 °C

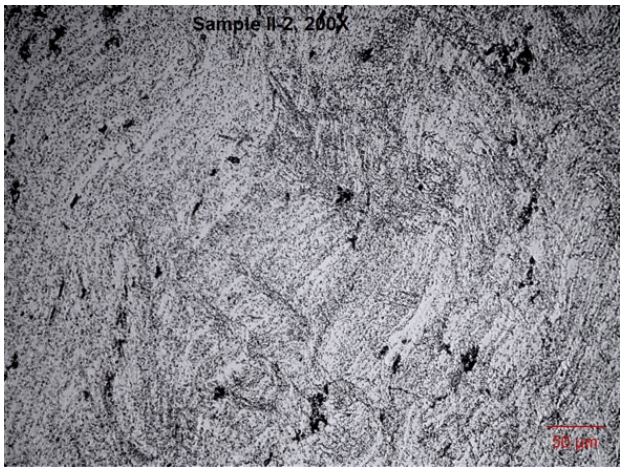

Fig. 6 Optical microstructure of the solution-treated material after 4(D) sc-ECAE passes at 250 °C

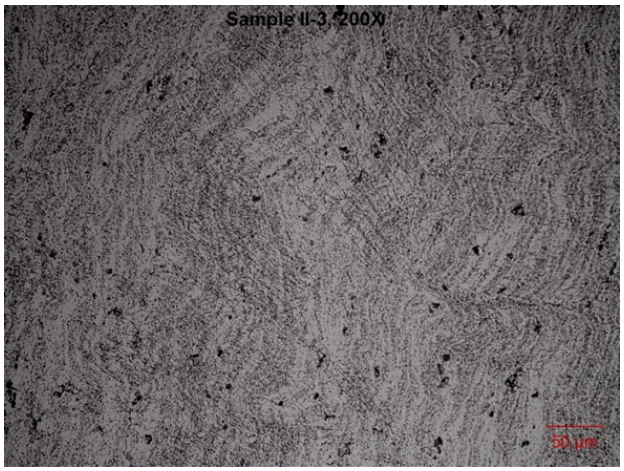

Fig. 7 Optical microstructure of the overaged material after 4(D) sc-ECAE passes at 250 °C

The microstructures of the sc-ECAE-processed samples were further examined by EBSD analysis. In general, for all three conditions their appearances were similar. Typical EBSD results are illustrated in Figs. 8a–c for the as-received condition. The estimated average refined grain size is about 1.2 μm. The misorientation angles for most of these grain boundaries are in the range of 2°–5°. Such low angle boundaries are characteristic of sub-grains rather than normal refined grains. The sub-grains occupy the larger parts of the old parent grains that have diffused high-angle boundaries. These data differ from the previous results for the AA5083 processed by discontinuous ECAE under identical conditions. That data showed the refined grain microstructures with an average size of about 0.4 μm, and the boundary misorientation angles for most of the grains were more than 12°.[3] For the solution-treated and overaged conditions, the misorientation angles are slightly lower than those shown in Fig. 8c. However, a post-ECAE processing examination of these two last cases did not detect any evidences of flow localization and surface cracks. The differences demonstrate that adiabatic heating during sc-ECAE was noticeable, and it affected the dynamic recrystallization and recovery processes.

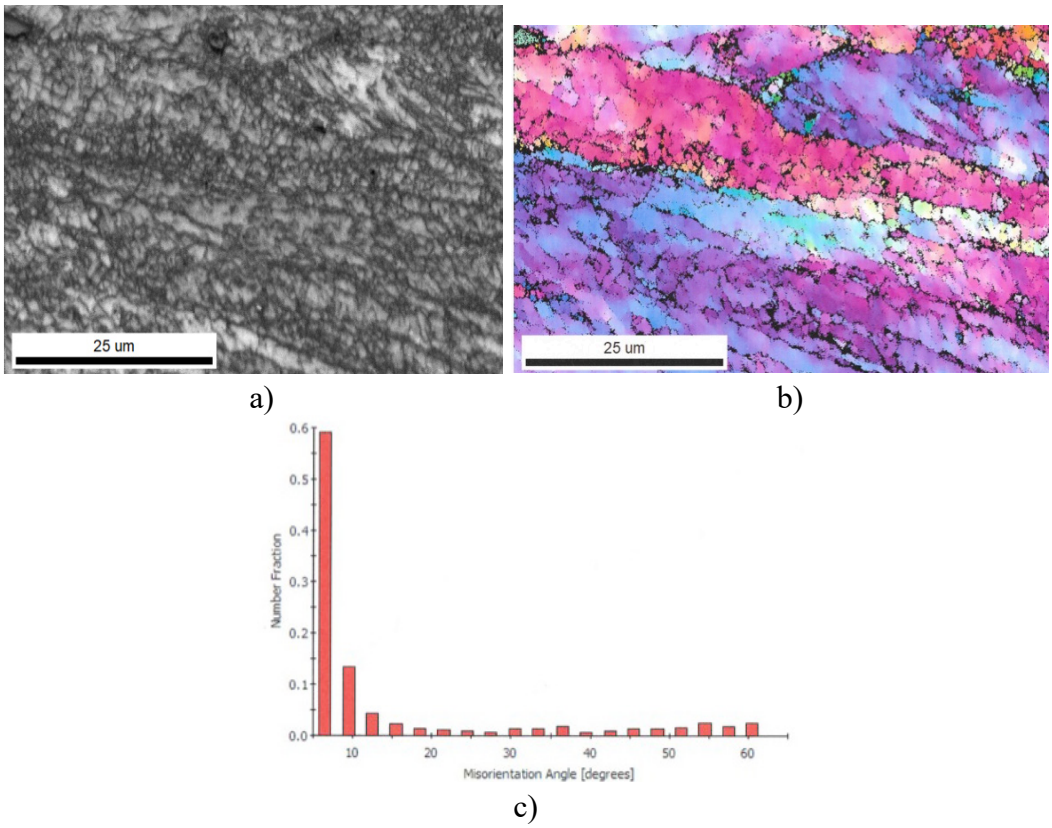

Fig. 8 EBSD analysis of the as-received material after sc-ECAE: a) image quality map (step size is 70 nm); b) color-coded orientation map; and c) misorientation angle histogram (5° is set as the minimum)

2.2.4 Rolling of sc-ECAE-Processed AA5083

Direct use of the large-scale slab-like billets after sc-ECAE may only find special and restricted applications whereas rolled products such as plates, sheets, and strips produced from these billets could find more applications in different industries. Therefore, subsequent rolling of the ECAE plate material is a necessary production step for commercialization of the ECAE technology and should be included in any evaluation of the final material properties.

After sc-ECAE, all 15- × 15- × 3.125-cm^3 samples were scalped to a 2.5-cm thickness and rolled at 150 °C using a rolling mill with a roll diameter of 40 cm. Samples for structural characterization and tensile testing were selected after thickness reductions of 50%, 75%, 87.5%, and 93.75%. Rolling up to and including an 87.5% reduction did not develop any defects. However, at a reduction of 93.75%, edge cracks were observed depending on the initial material conditions (Fig. 9). The biggest cracks were observed in the as-received material after 4(D) sc-ECAE passes (sample (a), #14), whereas the same but solution-treated material (sample (c), #24) did not lead to any edge cracks. This condition showed the best combination of workability and ductility; therefore, it was selected for more detailed analysis and for additional larger industrial-scale experiments.

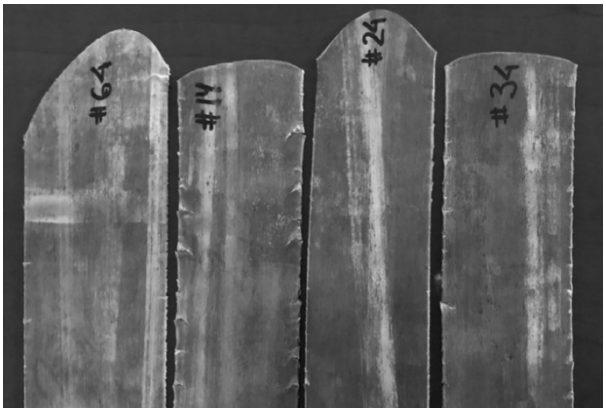

a) b) c) d)

Fig. 9 Edge cracks after reduction of 93.75%: a) as-received material; b) as-received material + 4(D) sc-ECAE passes; c) solution-treated material + 4(D) sc-ECAE passes; and d) overaged material + 4(D) sc-ECAE passes

Figure 10 shows a series of optical microstructures obtained after rolling of the solution-treated material to reductions of a) 50%, b) 75%, and c) 87.5%. As the amount of reduction increases, the isotropic microstructure (as was shown in Fig. 6) is transformed into a fine, strictly oriented laminate microstructure.

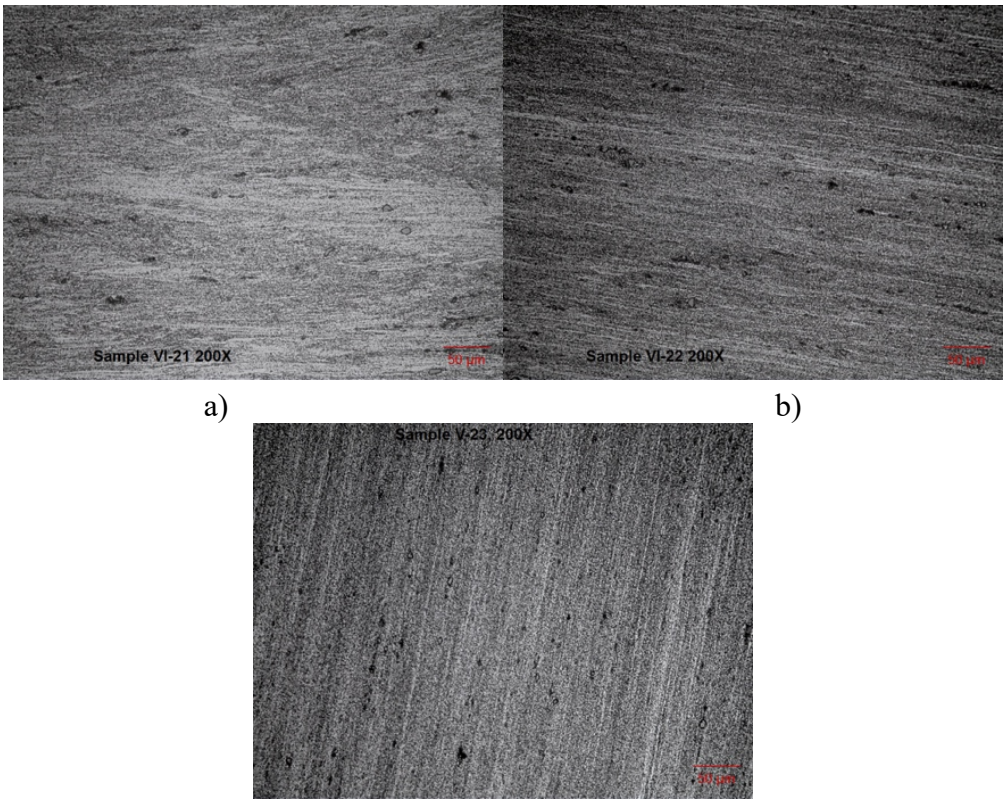

Fig. 10 Optical microstructures of the solution-treated material after rolling reductions of 50% in a), 75% in b), and 87.25% in c)

An important note should be made regarding the macro segregation of particles in AA5083. All sample cross sections including the original materials, materials after sc-ECAE, and materials after rolling reveal a narrow black region at their center. This area (Fig. 11a) reflects a variation in the chemical composition (i.e., macro-segregation) induced during ingot solidification, which cannot be eliminated by homogenization. The occurrence of this variation happens as follows. When the solidification fronts propagate from the plate edges toward the mid-thickness, they bring a depleted solution of some of the alloying additivities, which, as a result, form fewer dispersions. A microstructural analysis shows that the density of dispersions in the darker central area (Fig. 11a) is two to three times lower than in the outside areas. This area has a lower strength that may result in possible material delamination at the mid-thickness plane during rolling or ballistic testing (spall) of the ECAE armor material.[4]

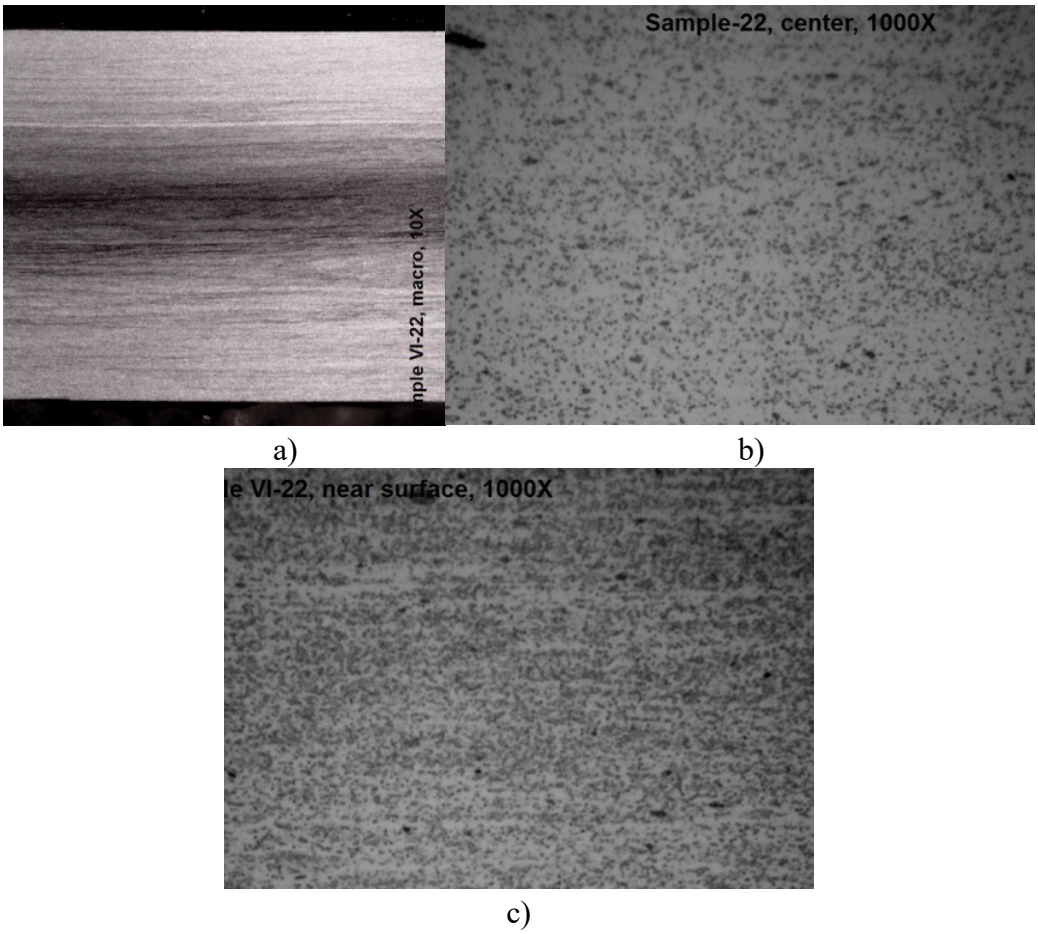

Fig. 11 Overview of mid-thickness segregation in the billet in (a, ×10), and intermetallic particle concentrations in the center (b, ×1000) and the off-center (c, ×1000) areas

Some data obtained from the EBSD analysis of the sc-ECAE-processed material after additional rolling with a reduction of 50% are presented in Fig. 12 for the as-received condition. A comparison with Fig. 8 shows that during rolling, the sub-grains that formed by sc-ECAE change from having an equiaxed morphology into thin elongated grains with an average size of about 0.4 μm, confirming intragranular dislocation glide and hardening. Also, note that the boundaries of the large original parent grains disappear, intermetallic particles are crushed/fractured into small pieces, and most low-angle boundaries are transformed into high-angle boundaries. The histogram in Fig. 12c shows that the high-angle boundaries (>15°) correspond to about 55% of all of the boundaries present.

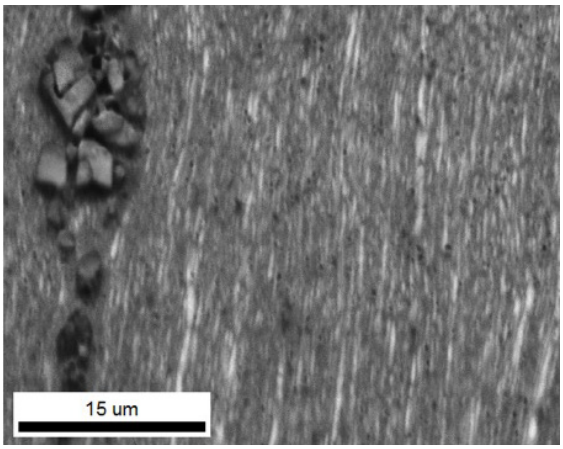

a)

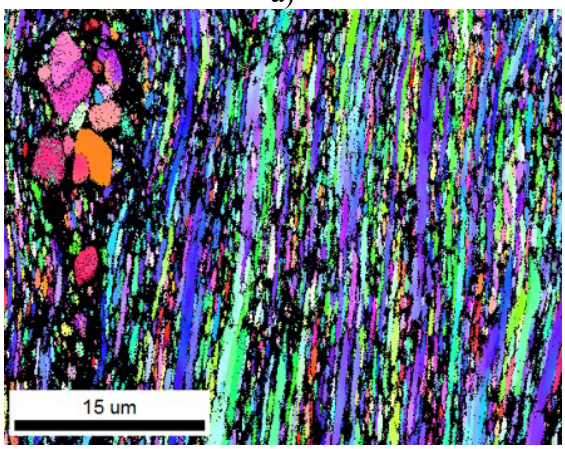

b)

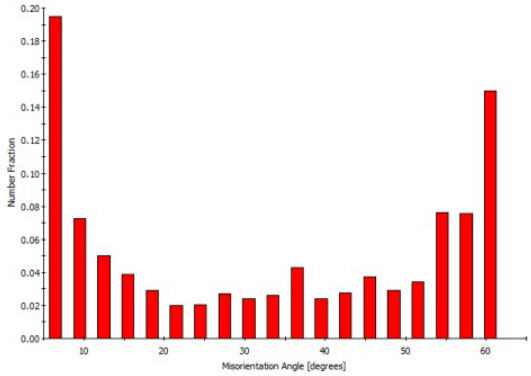

c)

Fig. 12 EBSD analyses of the as-received material after sc-ECAE + 50% rolling reduction: a) image quality map (step size is 25 nm); b) color-coded orientation map; and c) misorientation angle histogram (5° is set as the minimum)

2.2.5 Mechanical Properties

Figure 13 shows the effect of rolling reduction on the hardness of the AA5083 alloy for the original and different processing conditions: 1) as-received material without ECAE; 2) as-received material + overaging + 4(D) sc-ECAE passes; 3) as-received material + 4(D) sc-ECAE passes; and 4) as-received material + solution treatment + 4(D) sc-ECAE passes. Equidistance curves in Fig. 13 confirm that the basic mechanisms of strengthening during rolling are structural refinement and dislocation hardening regardless of processing conditions. The greatest increase and highest hardness was observed for the solution-treated material. Tensile tests were performed for this condition along the rolling direction. Results are presented in Fig. 14. For rolling reductions in the range from 75% to 85%, which are typical for the rolling of plate materials, practically achievable properties are yield stress (YS) > 430 MPa, ultimate tensile strength (UTS) > 465 MPa, and relative elongation (EL) ~ 15%–17%. For comparison, curve 4 in Fig. 14 shows a UTS for an identical discontinuous ECAE process, which is close to curve 2 for the semicontinuous ECAE process of the solution-treated material.

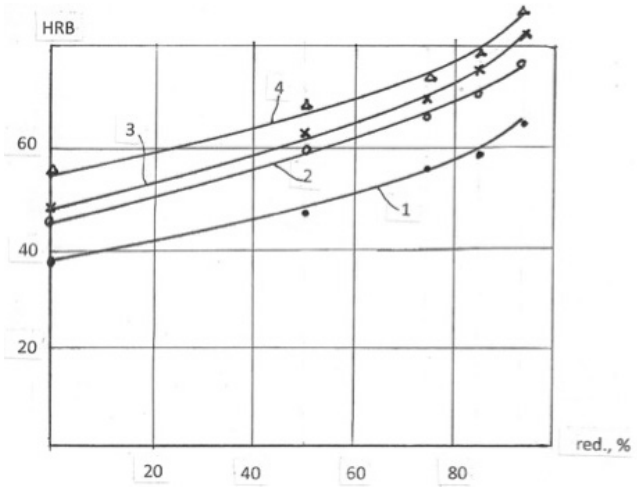

Fig. 13 Effect of rolling reduction on hardness: 1) as-received material; 2) as-received + overaged + 4(D) sc-ECAE passes; 3) as-received material + 4(D) sc-ECAE passes; and 4) as-received material + solution treated + 4(D) sc-ECAE passes

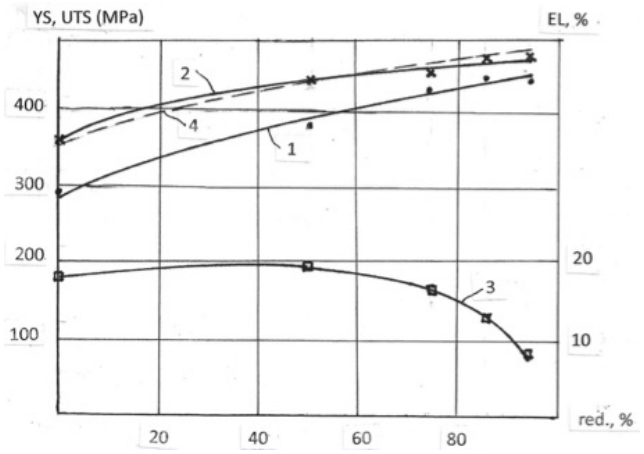

Fig. 14 Effect of rolling reduction on YS, UTS, and EL: 1) YS of the solution-treated condition; 2) UTS of the solution-treated condition; 3) EL of the solution-treated condition; and 4) UTS of discontinuous ECAE of the as-received material

It is informative to compare the mechanical properties of AA5083 achieved by different processing routes. Table 2 shows the YS, UTS, and EL obtained from samples taken from 1-inch plates of as-received AA5083 H321, AA5083 after 4(D) passes of ECAE at 250 °C, and the same material after solution heat treatment + 4(D) ECAE passes at 250 °C. The table also lists the mechanical properties of the rolled material after a reduction of 85%. In both cases, sc-ECAE provides a similar increase of the UTS (of about 16%) for the as-received and solution-treated material conditions. The additional increase of UTS by follow-up warm rolling is also identical for both cases. For a reduction of 85%, the strength increase is approximately 28%. In comparison with the ordinary as-rolled plate material AA5083 H321 without ECAE, the total improvement of the UTS is almost 50%. Also, by reducing the number of precipitates, the solution heat treatment of the original material significantly improves workability during ECAE, including ECAE at lower temperatures, and during subsequent rolling as well as ductility of the final material.

Table 2 Mechanical properties of AA5083 after various processing routes

Processing route	Yield stress (MPa)	Ult. tensile strength (MPa)	Elongation (%)
As-received AA5083 H321	228	317	22
As-received material after 4(D) ECAE	290	366	18
As-received material after solution treatment + 4(D) ECAE	296	370	18
As-received material after 4(D) passes of ECAE + warm rolling with reduction of 85%	450	475	10
As-received material + solution treatment + 4(D) passes of ECAE + rolling with reduction of 85%	455	470	14

The data in Table 2 indicate that post-ECAE rolling is not only a necessary step in the production route, but also an important step in the fabrication of high-strength lightweight materials.

2.3 Optimization of Semicontinuous ECAE of Magnesium Alloy AZ31

2.3.1 Microstructure Refinement

Historically, multipass ECAE at temperatures below the recrystallization temperature was first applied to aluminum alloys as a means to achieve structural refinement to a sub-micrometer grain size through the formation of new high-angle grain boundaries. Later, this approach was extended to magnesium alloys. However, in contrast to aluminum alloys that have a face-centered cubic crystallographic lattice, magnesium alloys having the hexagonal close-packed crystallographic structure are of much lower ductility and can be processed via severe plastic deformation only at temperatures well above the recrystallization temperature.

In principle, sub-micrometer structures in Mg alloys can also be achieved by ECAE at temperatures under the recrystallization temperatures with the application of high back-pressures. For example, the recrystallization temperature of AZ31 is 200 °C and, to suppress fracture during ECAE at lower temperatures, the magnitude of the back-pressure should be comparable to the material yield stress. This is highly impractical and difficult to realize at an industrial scale. In addition, rolling of the obtained Mg alloys after ECAE with back-pressure into plate and sheet products cannot be performed at such low temperatures because of heavy edge cracking,

whereas rolling at hot temperatures to eliminate cracking leads to the degradation of the as-processed sub-micrometer grained microstructure and properties.

On the other hand, Mg alloys are more readily disposed to dynamic recrystallization, which can take place at specific ranges of strains, strain rates, and temperatures. In a recent article, Vinogradov et al.[5] analyzed numerous papers on the severe plastic deformation processing of Mg alloys and demonstrated that in most cases dynamic recrystallization results in grain sizes less than 10 μm. Further optimization could potentially produce a minimum grain size of a few micrometers. As dynamic recrystallization depends strongly on recovery between passes, sc-ECAE is an effective processing technique for such optimization. This new concept was confirmed by subscale experiments on AZ31 for a billet size of 15 × 15 × 3.125 cm. The extrusion speed was 2 mm/s. The equivalent strain rate of about 0.5/s is comparable to the typical strain rates accessible on industrial hydraulic presses. The remaining variable parameters were the temperature and the number of ECAE passes necessary to achieve a stable, uniform, and minimum grain size. The results are discussed below.

Figure 15 shows a representative microstructure of the original AZ31 material. The grains are equiaxed with an average size of about 35 μm. ECAE processing was performed at temperatures of 200, 225, 250, 275, and 300 °C with one, two, and three passes, resulting in effective strains of 1.15, 2.3, and 3.45, respectively. Because of the significant grain size refinement, microstructures were detected on polished and etched samples by SEM at a magnification of 2000×. Selected results are presented in Figs. 16–21. One-pass ECAE was performed without cracks at 250 °C. It is worth noting that even a single pass dramatically changes the microstructure. At 225 °C, the microstructure (Fig. 16) is duplex, comprising a large number of very fine fully recrystallized grains with an average size of about 2 μm and some larger grains oriented in the shear direction. These heavily elongated grains are probably the remains of the much larger original parent grains. Similar results were observed for 250 °C (Fig. 17). For 275 °C (Fig. 18), the microstructure is totally different, with a few fine grains and a large number of recrystallized grains of 8–10 μm. This is due to the expected grain growth at elevated temperatures. Therefore, for a single ECAE pass, the optimal temperature is 250 °C. However, a single pass is not sufficient to complete the dynamic recrystallization process.

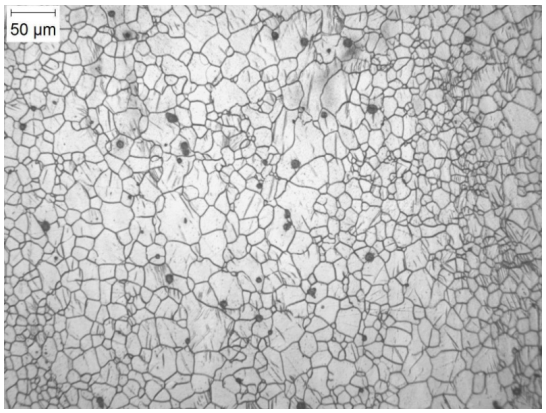

Fig. 15 Representative microstructure of the original as-received AZ31 material

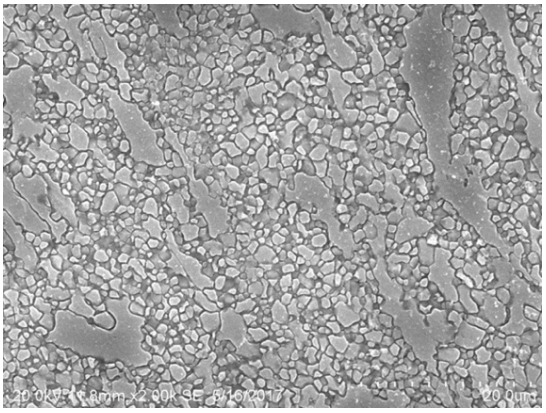

Fig. 16 Microstructure of AZ31 after one pass at 225 °C

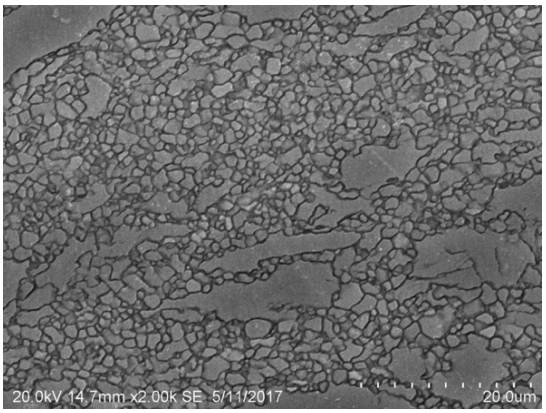

Fig. 17 Microstructure of AZ31 after one pass at 250 °C

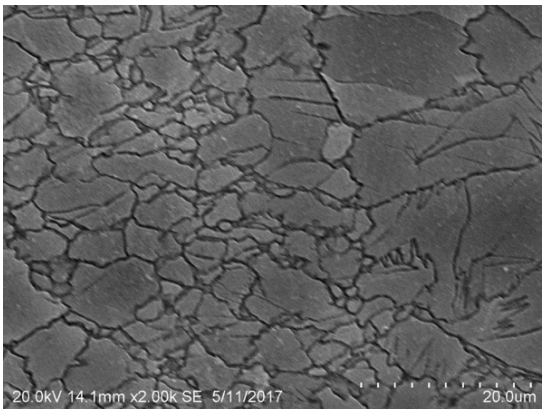

Fig. 18 Microstructure of AZ31 after one pass at 275 °C. Note the considerable larger grains compared to those at lower extrusion temperatures.

Two-pass ECAE processing was performed semicontinuously. No defects were observed at 250 °C. This temperature provided a better microstructure (Fig. 19) than the optimal microstructure after one pass at the same temperature (see Fig. 17). At 275 °C (Fig. 20), dynamic recrystallization of the bulk is completed. The previously observed duplex microstructure is absent, and a uniform, equiaxed, and ultrafine-grained microstructure with an average grain size of about 2 μm covers the entire material volume. Further increase of the temperature to 300 °C resulted in a duplex microstructure (Fig. 21).

Three ECAE passes were performed without defects at 300 °C but did not result in the further grain size refinement. Therefore, two ECAE passes at 275 °C was accepted as the optimal processing schedule for this material. It should be emphasized that for the equivalent, but discontinuous ECAE, similar grain size refinement was only obtained after four to eight passes.[5]

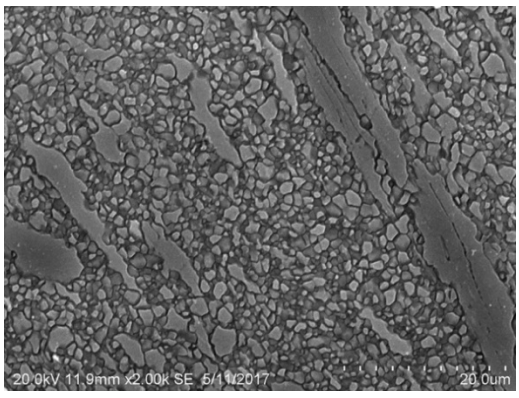

Fig. 19 Microstructure of AZ31 after two passes at 250 °C

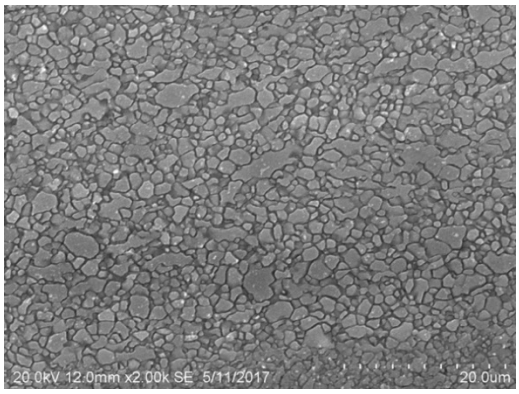

Fig. 20 Microstructure of AZ31 after two passes at 275 °C

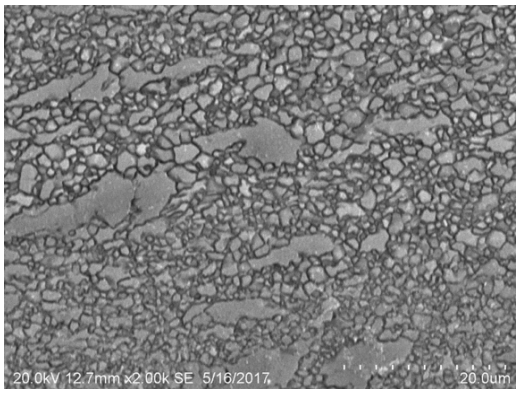

Fig. 21 Microstructure of AZ31 after two passes at 300 °C

2.3.2 Rolling of sc-ECAE-Processed AZ31 Material

Rolling of AZ31 was carried out at 300 °C on the same 40-cm mill used for the AA5083 rolling trials. Preliminary experiments showed that rolling at temperatures below 300 °C resulted in through-thickness cracks. The typical rolling schedule comprises a series of steps with partial reductions of 12% (or effective strains 0.14). After total reductions of 50%, 75%, 87.5%, and 93.75%, the material was reheated to 300 °C for 10 min. This schedule eliminated material cracks through the thickness of the plate as well as edge cracks. As the effective strains per rolling pass of 0.14 were lower than the similar strains of 1.15 per ECAE pass, and the preheating time was sufficiently long, the rolled material experienced repeated continuous recrystallizations between passes and discontinuous recrystallization during each reheating step. This resulted in a degradation of the ultrafine grain structure induced by ECAE and led to the development of more coarse microstructures.

Figures 22–25 show typical microstructures of AZ31 after rolling with reductions of 50% (Figs. 22, 24) and 87.5% (Figs. 23, 25), respectively, for two conditions: the original as-received material and the same material after two-pass ECAE, Route B, at 275 °C. In all cases, the microstructures after rolling are identical, comprising

fully recrystallized equiaxed grains with an average size of 7–9 μm at moderate reductions and 5–7 μm at high reductions.

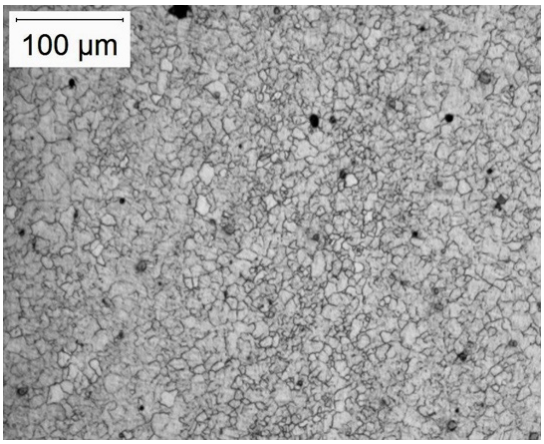

Fig. 22 Microstructure of the original AZ31 after 50% rolling reduction at 300 °C

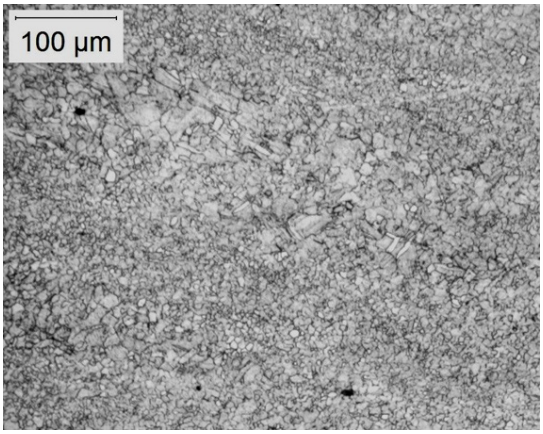

Fig. 23 Microstructure of the original AZ31 after 87.5% rolling reduction at 300 °C

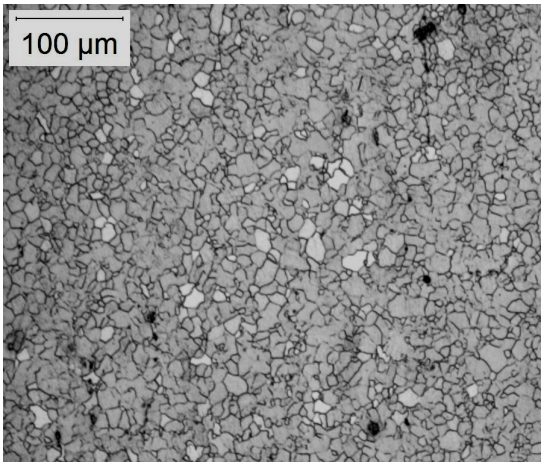

Fig. 24 Microstructure of AZ31 after 2(B) passes of sc-ECAE at 275 °C + 50% rolling reduction at 300 °C

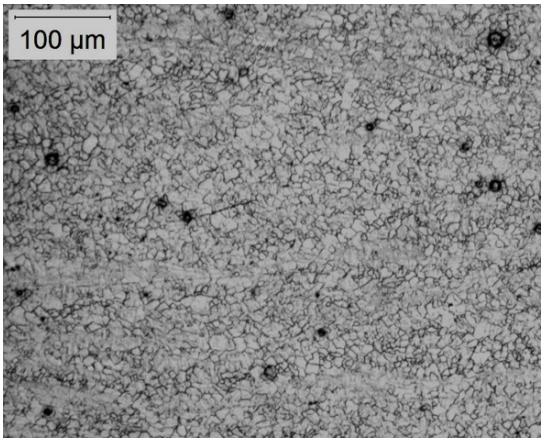

Fig. 25 Microstructure of AZ31 after 2(B) passes sc-ECAE at 275 °C + 87.5% rolling reduction at 300 °C

2.3.3 Mechanical Properties of AZ31

Table 3 presents the grain sizes and tensile properties of the alloy AZ31 after ECAE and ECAE + Rolling with different reductions. These data are compared with similar results for the as-received annealed material and the same materials after identical rolling. It is evident that sc-ECAE itself provides a noticeable improvement of material strength and ductility in comparison with both conditions of the original materials. However, in contrast to AA5083, additional rolling of the ECAE processed material does not provide any advantages against the ordinary AZ31 rolled products.

Table 3 Tensile properties of AZ31 in different conditions

Processing route	Average grain size (µm)	Yield stress (MPa)	Ultimate tensile strength (MPa)	Elongation (%)
Original annealed	35	140	248	22
Original annealed + rolling reduction:				
50%	13	200	278	19
75%	9	190	275	18
87.5%	8	165	275	16
93.75%	6	170	280	15
After 2(B) ECAE passes	2	240	335	28
After 2(B)passes ECAE + rolling reduction:				
50%	12	170	270	22
75%	8	210	280	17
87.5%	6	185	280	15
93.75%	6	180	282	13

These results demonstrate that compared with the original AZ31 alloy, ECAE increases the ultimate tensile strength by 35% and relative elongation by 25%. However, subsequent rolling of the material after ECAE leads to a degradation of the microstructure that renders the alloy properties to the same values as those obtained after rolling of the original material, giving rise to the question related to the rationale and expediency of such combined processing.

3. Large-Scale ECAE Tooling and Processing Approach

As detailed in a previous report (ARL-TR-8047[2]), numerous corrections and modifications were needed at the beginning of this effort to further increase the efficiency of the large-scale ECAE process. These changes can be separated into two categories: modifications to the tooling and the development of a DHS to ensure a uniform billet temperature during the extrusion process.

3.1 Tooling Die Modifications

Based upon the experience gained from the previous Phase II effort, the following corrections and/or modifications were made to the tooling die:

1) Increased the entering draft of the Vertical Die channel from 0.75 × 15° to 1.5 × 15°.
2) Reduced the clearance between the ring assembly and the bottom slider from 0.5 cm to 0.3 cm.
3) Cleaned and polished the Vertical Die channel.
4) Fixed the punch-channel clearance.

3.2 Tooling Die Heating System Modifications

3.2.1 Development of the Die Heating System

Results obtained from billets produced in the prior Phase II effort revealed that the temperature of the die plays an important role in ensuring a smooth extrusion process. Originally, it was assumed that the large mass of the tooling die would retain its temperature after it was heated overnight in a furnace. However, this was not the case. Indeed, the most serious problem during the previous forging runs was the inability to control and maintain a uniform die temperature. As a consequence, this resulted in the billet cooling between passes and subsequently developing edge cracks.

Prior experiments using the small-scale EPM die demonstrated that the die temperature should be more than 175 °C. Thus, before the second series of actual extrusion efforts began, an automated DHS was developed and incorporated into the die assembly. The system design and implementation was performed by Briggs Industries Inc., Chesterfield, Michigan, in cooperation with EPM. A system power of 80 kW was calculated for the heating of the heavy die to the required temperature of 200 °C for 6 h. Heating was provided by 40 cartridge heaters. As necessary, the holes and wiring channels were machined into the die inserts on opposite sides of the billet vertical input channel are shown in Fig. 26 (with the top covers removed). The heaters were arranged into four quadrant zones that could be independently controlled. As shown in Fig. 27, the fully assembled DHS with the auxiliary temperature control box and power supply cables was tested prior to ECAE processing. The ECAE tool inside the 11,000-ton press and the auxiliary operating system are shown in Fig. 28 during one of the forging runs at ETF.

Fig. 26 The redesigned tool with the new DHS (without the covers in place; the thermal insulation and tops and electrical connections to the heater cartridges can be seen)

Fig. 27 Testing the DHS

Fig. 28 Fully assembled large-scale ECAE die with the DHS at the 11,000-ton Ellwood press

3.2.2 Testing the Die Heating System

As stated earlier, the most serious problem during the previous forging runs was the inability to control and maintain a uniform die temperature. Experiments using the small-scale EPM die demonstrated that the die temperature should be more than 175 °C to prevent edge cracks. Prior to the forcing runs, the DHS was tested in a stand-alone mode as well as at the press. Testing protocols and resultant data for the latter case are shown in Table 4.

For the stand-alone die heating tests, a set-point temperature of 350 °C was used. Testing was conducted for 10 h and die temperatures were recorded at 30-min intervals in all four of the die heating zones and at the top and the mid-length of the vertical channel wall. In this test, the stationary temperature of the set point was practically attained in about 6.5 h, with the lowest temperature of the channel wall about 220 °C, a value that is well above the acceptable temperature of 175 °C.

Testing of the DHS confirmed that the system fulfilled the requirement for temperature uniformity in the die. However, the first production run showed that some of the cartridges were exposed to overheating and, in the future, should be replaced by more robust heavy-duty series cartridges.

Table 4 Testing protocols and data for the DHS at the 11,000-ton Ellwood press

Hour	Time	Temperature (°C)				Temp check with gun	
		Zone 1	Zone 2	Zone 3	Zone 4	Top of slot	Mid cavity
1	9 am	202	204	153	218	87	73
1.5	9:30 am	245	247	187	257	122	109
2	10 am	274	276	211	284	143	124
2.5	10:30 am	309	312	240	316	174	153
3	11 am	338	341	263	343	191	171
3.5	11:30 am	351	350	281	350	209	208
4	12 pm	351	350	305	350	227	202
4.5	12:30 pm	350	350	316	350	234	193
5	1 pm	350	350	331	350	238	217
5.5	1:30 pm	350	350	338	350	242	218
6	2 pm	350	350	343	350	246	213
6.5	2:30 pm	350	350	351	350	248	223
7	3 pm	350	350	350	350	246	221
7.5	3:30 pm	350	350	350	350	252	224
8	4 pm	350	350	350	350	253	218
8.5	4:30 pm	350	350	350	350	253	203
9	5 pm	350	350	350	350	256	221
9.5	5:30 pm	350	350	350	350	255	224
10	6 pm	350	350	350	350	257	226

Note: Heating system was turned on at 8:00 am; set point was 350 °C. The green shading is used to clearly mark the times at which the respective zones were at/above the set point.

3.2.3 ECAE Processing Modifications

Similarly, previous efforts also revealed issues associated with billet handling during the large-scale ECAE process. One of the most important modifications was the machining of special tips for the grips of the GLAMA manipulator at the Ellwood facility. The GLAMA is a rail-bound mechanized forging manipulator that is used to manipulate hot metal during a typical forging operation. In its original form, the single mandible grip proved ineffective at picking up the smaller ECAE billets used in this study. The attachment of the special tips resulted in a much improved gripping ability for the manipulator in these efforts. In addition, a ball table with adjustable stops was also manufactured and used during the extrusion process. The ability to adjust the stops on the table allowed for easier rotation and reorientation of the billet after each pass. In addition, the creation of excessive punch flash was also eliminated, which further served to improve billet handling. Finally, the procedures for both billet and die lubrication were also improved. Together, these changes resulted in the processing time between passes being reduced to less than 1 min.

3.3 Large-Scale ECAE Processing of AA5083 Billets

Three 60 × 60 × 10 cm^3 AA5083 billets were successfully processed in a semicontinuous manner for four passes via Route D (or Bc) at 250 °C. The typical billet appearance is illustrated in Fig. 29. The values of the maximum press load during each pass are shown in Table 5. The data show that the required load is significantly less than the press capacity. One can also see that semicontinuous ECAE is accompanied by an increase of the billet temperature, as indicated by a decrease of the press load at each subsequent pass.

Fig. 29 ECAE-processed AA5083 billet

Table 5 Maximum press load during four passes ECAE of AA5083

Pass	1	2	3	4
Maximum press load, t	2934	2390	2204	2105

3.4 Rolling of ECAE-Processed Billets: AA5083

The billets after large-scale ECAE are thick plates whose mechanical behavior approximates an ideal rigid plastic material. The critical rolling parameter in this case, known as the shape factor, is the ratio of the initial billet thickness (H) to that of the contact length (L) along the circumference of the roller.[6] For H/L less than 1, rolling does not lead to defects through the material thickness. However, for H/L greater than 1, central bursts and a split of the front billet end (also known as alligatoring) can be observed. The metallurgical factors for the development of such

defects are the inability of the deformation to penetrate through the entire thickness of the slab and the size and concentration of hard particles in the material. Therefore, for each material, there exists a maximum ratio $(H/L)_{max}$ for rolling without defects. In that case, the shape factor H/L can also be defined by the relative roll radius R/H, where R is the roll radius and the reduction of the material thickness per pass, e, is given by $(1 – h/H) \times 100\%$, where h is the thickness of the billet after each pass. To reduce roll pressure and provide a stable processing condition, the preferable reductions per pass are usually less than 10% and more typically are on the order of 5%–7%.

For thick plates of high-strength aluminum alloys like the ECAE-processed AA5083, alligatoring failure during rolling presents the biggest problems. From our previous experience during the earlier Phase II project, rolling of the as-received AA5083 plate after ECAE processing (plate thickness of 6.75 cm) on rolls with a diameter (2R) of 97.5 cm (H/R = 0.137) with reductions 5%–7% detected one case of alligatoring out of five billets. During the Phase II Continuation project, the material workability was substantially improved owing to the solution treatment due to the more uniform distribution and size of precipitates and dispersoids. Rolling of the solutionized subscale billets with a thickness of 2.5 cm using a roll diameter of 40 cm (H/R = 0.125) did not develop any defects (see Fig. 9). The actual ratio is probably close to $(H/R)_{max} = 0.13$. Therefore, for a billet thickness of 9.375 cm after ECAE and scalping, the required roll diameter should be D = 145 cm. Such large rolling mills do exist and operate continuously in industrial settings, but they are very expensive and are not available for experimental research–type works. After an intensive search, EPM was able to locate a suitable mill at the Manufacturing Science Corporation, located in Oak Ridge, Tennessee. This is a two-stand reversible mill with roll diameters of 47 cm and automated control of the rolling gap. The company has experience rolling various alloys.

Two AA5083 billets (56.82 × 52.71 × 9.19 cm, H/R = 0.39) were shipped for rolling. Billets were preheated to 150 °C. The first billet rolled with a reduction of 12% showed heavy alligatoring and could not be used for additional processing (Fig. 30). The second billet rolled with a reduction of 5% detected alligatoring at the beginning and rolling was stopped. The front end of the billet was then removed and the remaining part was separated into three pieces, machined to thicknesses of 3.75, 5, and 6.25 cm, respectively. The rolling experiments were then continued for the following three samples:

- Sample 1 (35 × 16.875 × 3.75 cm, H/R = 0.16);
- Sample 2 (35 × 16.875 × 5 cm, H/R = 0.22); and
- Sample 3 (35 × 16.875 × 6.25 cm, H/R = 0.27).

Fig. 30 Alligatoring of a full-scale large billet of AA5083 during rolling

Samples 1 and 2 were rolled with a reduction of 5%. After a few passes, both samples showed front-end splitting and the rolling was stopped (Fig. 31). Sample 3 was rolled with a reduction of 12.5% and also showed a front-end split (Fig. 32). These experiments demonstrated and confirmed that rolling of the large-scale ECAE material required rolling mills with larger roll diameters.

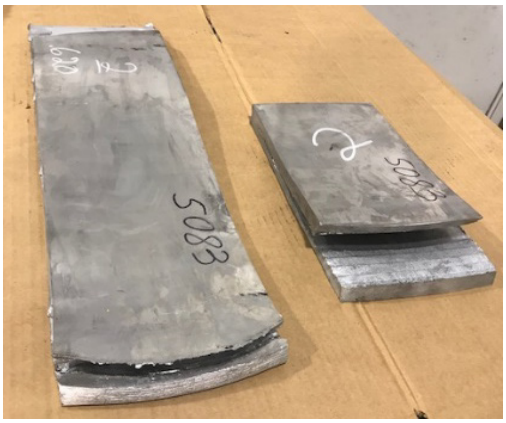

Fig. 31 Alligatoring of sample 2

Fig. 32 Alligatoring of sample 3

To avoid this complexity, it was suggested that a technique known as roll forging–reverse rolling be used to produce the desired plates. In this case, the gap between the rolls was open such that the preheated plate billet could be placed between the rolls. The top roll was then lowered and used to forge the plate to the desired thickness after which point reverse rolling was performed, first in one direction and then in the opposite direction. In this way, both billet ends were protected from splitting. Figure 33 demonstrates roll forging–reverse rolling for sample 1. The previously induced split end was cut off, and the remaining part was successfully rolled to a thickness of 0.745 cm, resulting in a total reduction of 80% without any further problems. Such an approach is simple and practical and can be used in any follow-up work.

Fig. 33 Rolling of sample 1

3.5 Large-Scale ECAE Processing of AZ31 Billets

Originally, it was intended that two AZ31 billets would be subjected to large-scale ECAE processing. However, several deep cracks were observed in the first billet after the first pass. Thus, this billet could not be used for further processing. An inspection of the second billet showed only a few small cracks at the front end. This end was cut off, and the billet was subsequently approved for continued processing. The cracks were caused by unexpected failure and shut down of two zones of the DHS that resulted in the nonuniform cooling of the die. Therefore, prior to the second pass of the second billet, the heating zones were repaired, and the die was allowed to come to a uniform temperature. Prior to any future work, the DHS should be modified and inspected for its reliability.

3.6 Rolling of the ECAE-Processed AZ31 Billets

Because of the experience with AA5083, the two-pass magnesium alloy billet was separated into 20.575- × 37.8- × 8.9-cm pieces and shipped for rolling. Before rolling, both pieces were preheated to 300 °C. The first piece rolled with a 10%

reduction revealed numerous surface and through-thickness fractures (Fig. 34). Therefore, the second piece was processed by the roll forge–reverse rolling technique. Partial 5% reductions were used during rolling to the final material thicknesses of 5, 2.5, and 1.3 cm with intermediate preheating. The final plate size of 200 × 56.875 × 1.3 cm was rolled without defects.

Fig. 34 Fracture of AZ31 after rolling

4. Automation Concept for Large-Scale ECAE Operations

4.1 Introduction

Among the various known techniques of severe plastic deformation, ECAE has the greatest potential for industrial upscaling and applications, provided it can be transitioned into a manufacturing environment on the industrial scale in a cost-effective manner. Large-scale ECAE of plate-shaped billets presents such an opportunity for further fabrication of rolled plates and sheets. In addition, as it will be shown in the following sections, semicontinuous ECAE can be performed on automated lines at specialized production plants. The incoming raw material should be in the form of large plates of 7.5–15 cm thickness supplied by metallurgical plants. Separating the plates for specific-sized blanks does not present any technical problems. The key phase of the overall process is the multistep, semicontinuous ECAE at the press, which is an integral component of the automation lines. The ensuing steps of scalping and rolling of the ECAE-processed billets are also ordinary and common technological operations at the corresponding equipment. Therefore, this part of the report is mainly focused on the conceptual development of the ECAE automation line.

4.2 An Analysis of Large-Scale ECAE at ETF

4.2.1 Layout of the Processing Area

Figure 35 shows the top view schematic floor plan of the processing area at the ETF plant. The ECAE tool is mounted at the 11,000-ton forging press equipped with a rail manipulator, which is not shown in the drawing. The manipulator delivers the preheated billets from the oven to the press, inserts the billet into the die, and performs all of the handling operations during the multipass ECAE process. During the extrusion trials at ETF, the transfer of the billet after ejection from the die to the rotational table, the 90° rotation of the billet at the table, and the lubrication of the billet and the die were all performed manually.

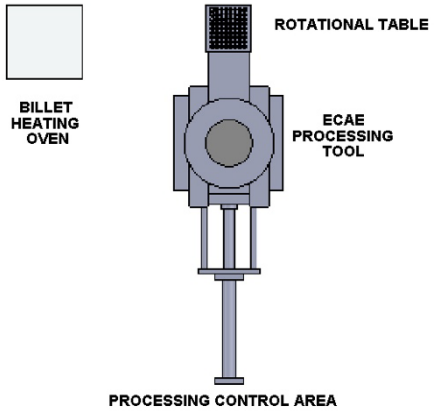

Fig. 35 Floor plan of the processing area at ETF

The specific handling operations are detailed and shown in Fig. 36: 1) manual billet lubrication, preheating in the oven, and delivery of the billet by the manipulator from the oven to the press; 2) manual lubrication of the billet and subsequent insertion into the die channel by the manipulator; 3) manual channel lubrication and subsequent billet extrusion and ejection from the die using the press; 4) manual billet rotation at the ball table; and 5) delivery of the billet by the manipulator to the cooling area after the completion of the required number of passes.

This sequence of steps and the use of the processing and auxiliary devices were dictated by the necessity to adapt to the existing forging equipment at the ETF plant that had limited options for automated or mechanized billet handling. For this reason, the ECAE processing at ETF required extensive manpower to assist with the billet transfer and orientation, billet and die lubrication, and control of the processing parameters. All of these operations were rehearsed, timed, then fixed, and subsequently analyzed to iteratively improve and, in turn, develop the optimal strategy for automatization.

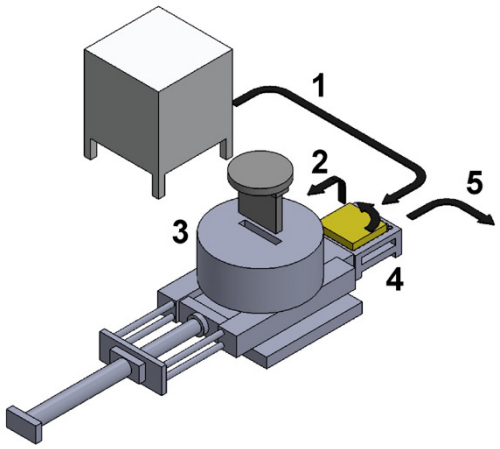

Fig. 36 Billet-handling operations at ETF

4.2.2 Breakdown and Analysis of the Operations

Table 6 presents the sequence, timing and labor, and equipment required for all of the operation steps. Note, steps 1–12 are repeated per pass.

Table 6 Description and characterization of the ECAE operations

No.	Operational Step	Time (s)	Assist. persons	Equipment
1	Billet lubrication and loading in oven	120	2	Forklift
2	Billet transfer from oven to press	60	2	Forklift, manipulator
3	Billet lubrication	30	2	Manipulator
4	Die lubrication	30	1	By hand
5	Billet insertion	20	2	Manipulator
6	Extrusion	80	1	Press
7	Billet ejection	40	2	Press, cylinder
8	Billet rotation	20	1	Rotation table
10	Billet clamping by manipulator	20	2	Manipulator
11	Billet, die lubrication	30	2	By hand
12	Billet inserting in the die for next pass	20	2	Manipulator
13	Billet transfer to the cooling area	30	2	Manipulator

With some of the steps being performed simultaneously, the total time for one pass including the billet delivery to the press is about 5 min. Correspondingly, four-pass ECAE takes about 20 min. On one hand, this means that the actual extrusion time comprises only about 25% of the total time, whereas 75% of the total time must be spent with secondary operations. On the other hand, nine press crew members were necessary to provide the required support for the experimental forging runs at ETF. Obviously, such low productivity rates and high labor cost cannot be accepted by

industrial operations. The extrusion time is defined by specific temperature–strain –strain rate processing conditions for each material type and is fixed. Therefore, the practical way to transition this technology is to significantly reduce the handling time and introduce automation, whereby the need for manpower is minimized. The following concept of an ECAE automation line addresses and resolves both of these problems.

4.3 The ECAE Automation Line

4.3.1 General Concepts

Figure 37 shows the conceptual design of the ECAE automation line. For simplicity, the press is not shown. The automation line includes the following units: preheating conveyor oven, billet transferring unit conveyor, nesting table, robot, billet lubrication chamber, channel lubrication unit, ECAE tool, and out-feed conveyor. Each unit will be described in following sections. The floor plan view of the line is shown in Fig. 38.

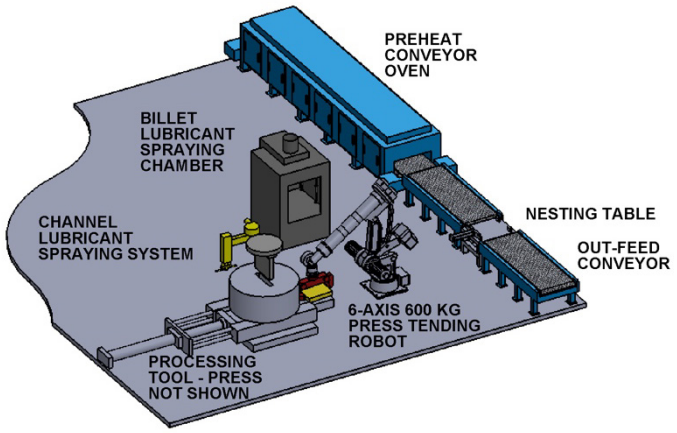

Fig. 37 Concept of the ECAE automation line mounted at the forging press

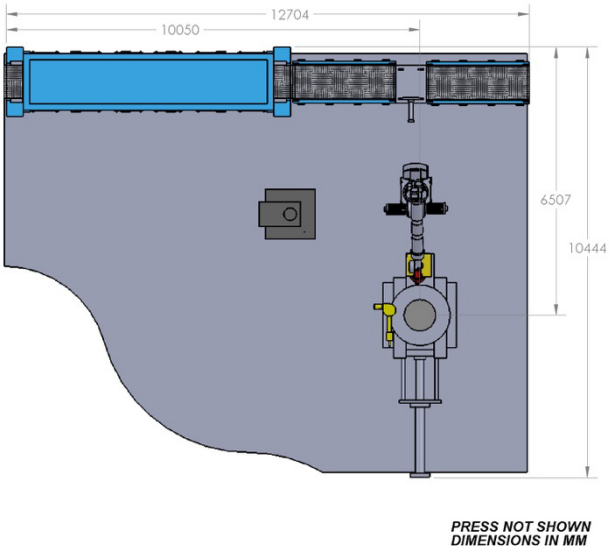

Fig. 38 Top-down view of the ECAE automation line

4.3.2 Material Flow

Original blanks of the required-size material are loaded onto the oven conveyor. At the output conveyer end, the preheated billets are periodically transferred to the speed conveyer, which delivers billets to the nested table. At the table, the billet position is fixed in two horizontal directions by stops and a pneumatic cylinder. In this position, the billet is clamped, picked up, and transferred by a robot to the spray lubrication chamber. Simultaneously, the die channel is lubricated by the channel spray lubrication system. Subsequently, the robot inserts the billet into the channel, releases it, and returns to its original position. Then the press extrudes and ejects the billet into the position shown in Fig. 37. The robot clamps, picks up, and transfers the billet again to the lubrication station. This procedure is repeated the required number of times. After the last pass, the robot transfers the fully processed billet to the out-feed conveyor. The six-axis robot is programmed to provide the correct billet orientations between passes and positioning in accordance with the overall processing protocols. Once the processed billet is on the out-feed conveyor, the next billet is released from the oven onto the oven conveyor.

4.3.3 Preheating Oven

In our opinion, the optimal preheating equipment is an infrared radiant oven with an internal horizontal flat metal chain conveyor (blue rectangle in Fig. 38, larger view in Fig. 39). The conveyor is indexing and can work continuously or in start/stop mode with variable speed. Loading of the billets on the conveyor can be done by forklift or automatically, if there is a special rack system available for the delivery of the blanks. It is expected that the preheated billets are periodically

drawn out from the oven and placed onto the speed conveyor, which delivers billets to the nesting table. Characteristics of the oven calculated for billets 60 × 60 × 10 cm and for the production of six billets/h are shown in Table 7.

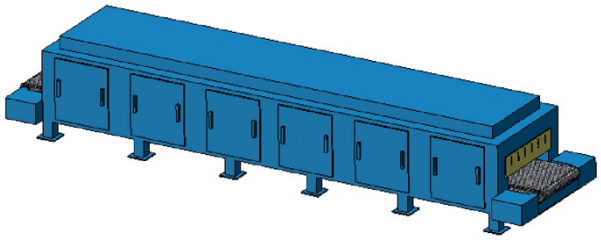

Fig. 39 Preheating oven

Table 7 Calculated characteristics of the oven

Billet dimensions	60 × 60 × 10 cm
Billet weight	100 kg
Hourly production rate	0.6 ton/h
Hourly throughput in billets	6
Billet heating time	1 h
Quantity of billets in oven	6
Gap between billets within oven	60 cm
Length of the heating zone	5.5 m
Conveyor length	6.1 m
Average conveyor speed	0.1 m/min
Heating power	250 kW

4.3.4 Billet Transferring Conveyors

For transferring the billets to the processing area and later from the processing area to the cooling and packaging area, regular chain conveyors are used (Fig. 40). The first in-feed conveyor promptly delivers billets to the nesting table. The length of this conveyor can be from 1.25 to 1.80 m, a length that provides good access to all of the line units during service and repair works. The nesting table provides an accurate interface between the robot and the in-feed conveyer necessary for billet insertion into the die channel with an accuracy within an allowance of 6 mm. Fixed stops and a pneumatic pushing cylinder secure the billet into the correct position at the nesting table. The operational sequences of the conveyors, robot arm, and nesting unit are controlled by a central programmable logic controller (PLC).

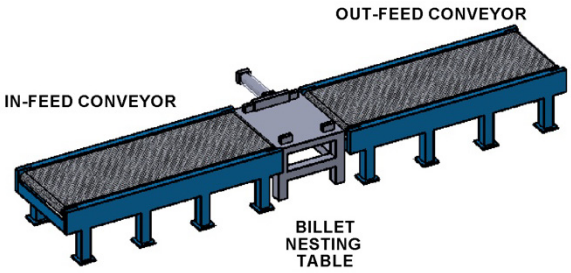

Fig. 40 Conveyors and nesting table

4.3.5 Robots

A robot will be providing all handling operations with high speed and accuracy. Robot suppliers offer an extensive selection of this type of unit with various characteristics for payload, reach distances, and axis control. For a billet weight of 100 kg and related clamping system, actuators, and drives, the required payload was estimated at 600 kg. Based on data given in the specifications of several robots capable of the same payload, the reach distances for the horizontal and vertical radii are 3000 mm. The minimal distance for which the robot arm can still operate is 1400 mm from the swirl axis of the robot. Therefore, the width and height of the working zone are 1600 mm and 3000 mm, respectively. This space allows the robot to manipulate freely with objects up to 1000 mm long and wide. The vertical reach of 3000 mm is also high enough for billet insertion into the die, which is 2000 mm high. Figure 41 shows the robot model of the calculated capacity. The axis legend is based on the YASKAVA approach (Yaskava America Inc., Buffalo Grove, Illinois). The designations of S, L, and R are basic axes providing movement all around the working zone. More advanced robots have additional axes for better accommodation of complex tooling and positioning. A six-axis robot would simplify the critical operation phase of the overall process, which entails the ECAE processing including a billet rotation of 90° after each pass.

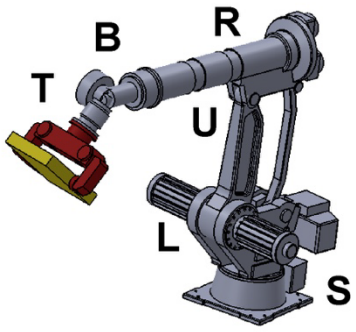

MAXIMUM PAYLOAD [kg]	600
HORIZONTAL REACH [mm]	APP 3000
VERTICAL REACH [mm]	APP 3000
CONTROLLED AXES	6

AXES LEGEND (YASKAWA)

S	SWIVEL
L	LOWER ARM
U	UPPER ARM
R	ARM ROLL
B	WRIST BEND
T	TOOL FLANGE

Fig. 41 Robot

4.3.6 Billet/Tool Lubrication

Lubrication of the billet and die channel is performed by automated spray systems. Presently, this technique is well developed and understood in the forging industry. In the first case, the billet is placed by the manipulator (see Fig. 36) into a special chamber (Fig. 42) with spraying nozzles before each pass. In the second case, a special robot (Fig. 43) mounted at the die (see Fig. 36) periodically rotates toward the vertical channel die axis and moves the arm of nozzles along its vertical axes, spraying lubricant. Also, the die is provided with a heavy grease lubrication system to deliver the anti-seize lubricant to the slider guide plate.

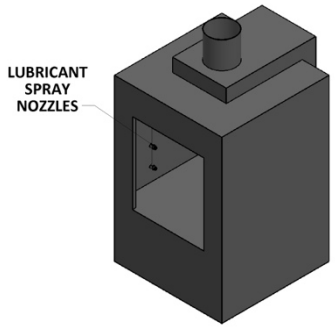

Fig. 42 Billet lubrication chamber

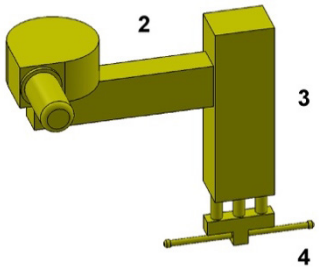

Fig. 43 Channel lubrication robot

4.3.7 Control System

An integrated PLC control system of the ECAE automation line includes a press control system, a die heating temperature control system, two robot control systems, a heating oven control system, two conveyor control systems, a billet lubrication chamber control system, a die cylinder control system, and a nesting table control system. These systems are equipped with actuators, drives, and the necessary sensors of positioning, temperature, pressure, and speed. The integrated PLC provides the oversight for the required sequence and correct performance of all units and their operations.

4.3.8 Technical Characteristics and Economic Factors

The overall productivity of the ECAE automation line is defined by two factors: the main operational time—that is, the time required for the extrusion processing—and the subsidiary operational time for the steps that also need to be performed. According to the present research, a single pass of ECAE requires 80 s, regardless of the scale. Assuming that each of the subsidiary operations at the automation line requires 60 s, four ECAE passes takes a total of 9.33 min. With a production rate of six billets/h, that translates into 24,000 billets/year (two shifts × 250 working days), or 2,400 tons/year of AA5083.

Once the automation is implemented, it is expected that the required manpower is three technicians—specifically, one technician for operating the heating oven area, one for operating the conveyor-robot–press area, and one for operating the cooling/packaging area for the processed billets. Note, these approximate characteristics can be adjusted and improved for higher productivity quotas.

5. Conclusions

The general goals of the Phase II Continuation project were 1) the development and demonstration of a large-scale, high-volume processing technology and 2) identification of the industrial methods/techniques based on semicontinuous ECAE processing and rolling of lightweight metals. The representative materials selected were AA5083 and magnesium alloy AZ31.

Regarding the overall program, several conclusions can be drawn. These are related to the characteristics of the representative lightweight materials, aspects of the semicontinuous ECAE technique, the upscaling of the methodology to a larger scale, a description of the required tolling, and the concepts for transitioning it into an automated manufacturing environment.

AA5083

- Identified the key steps and characteristics in the multipass ECAE processing of AA5083 for subsequent rolling of plate products. The best results were obtained for the original material that was solution treated at high temperatures providing a full dissolution of the as-formed precipitates and some dispersions. The optimal number of ECAE passes is four at a temperature of 225–250 °C, which results in a uniform microstructure of subgrains with an average size of about 1.2 µm.
- Subsequent rolling at 150 °C refines the microstructure further and transforms most of the subgrains into grains with an average size of about

0.4 μm. Rolling to a high reduction of 93.75% at a rolling mill with a sufficiently large ratio of the roll diameter to material thickness did not develop any defects, such as alligatoring through the thickness or the formation of surface or edge cracks.

- In comparison with the as-received baseline material having an ordinary temper of H321, the estimated increase of the strength of the ECAE armor-grade AA5083 plate material with a thickness of 2.5 cm is about 50%.

AZ31

- Identified the key steps and characteristics of the semicontinuous ECAE processing of a commercial magnesium alloy AZ31. Two-pass ECAE at 275 °C provides an average grain size of about 2 μm. The same grain size reduction using discontinuous ECAE that was previously obtained required 6–8 equivalent passes.
- Subsequent rolling without defects of ECAE-processed AZ31 alloy is possible only at a temperature at or above 300 °C. This rolling temperature results in the substantial increase of the grain size and concurrent degradation of mechanical properties.
- In comparison to the original as-received AZ31 alloy, ECAE increases the ultimate tensile strength by 35% and ductility by 25%. However, additional rolling of the ECAE-processed material leads to the degradation of the structure and properties, which prompts the question about practical expediency of such combined processing.

The second part of the program yielded the following results:

Large-Scale Tooling

- The large-scale die constructed in the previous Phase II program was restored, and its functioning was corrected for semicontinuous ECAE operations.
- An automated DHS was designed, tested, and implemented.
- The ETF forging line using the 11,000-ton press was upgraded with modified manipulator having grips, a ball table, and billet lubrication station to improve billet processing.
- Despite limitations of the facility, large-scale semicontinuous ECAE was implemented and practically realized at ETF in Houston, Texas.

Semicontinuous ECAE and Rolling

- Large-scale semicontinuous ECAE of AA5083 using an industrial die with an automated heating system was successfully demonstrated. Four passes were performed without defects and resulted in a material with a good surface finish.
- Large-scale semicontinuous ECAE of AZ31 was not fully successful because of the failure of the DHS during extrusion. After restoration of the heating system, a second billet was processed successfully under isothermal conditions.
- A problem was encountered during rolling of the large-scale ECAE billets of both alloys. Due to inaccessibility to rolling mills with large roll diameters, rolling was performed at a mill facility with a moderate diameter and a small ratio of roll diameter to billet thickness. Despite many attempts, rolling led to heavy alligatoring for AA5083 and through-thickness fracture for AZ31.
- Finally, a new concept of material forging between rolls followed by reverse rolling into both directions was developed and successfully tested, allowing a delivery of large-scale plate samples to ARL.
- The positive results and experience accrued during this Phase II continuation project provide solid evidence for the further development of a fully automated production line for semicontinuous ECAE of bulk billets.
- A conceptual design of the semicontinuous ECAE automated line was suggested and presented.

6. Suggestions for Future Work

There are two scenarios for the practical applications of semicontinuous ECAE. For relatively small billets and a low-volume production, ECAE can be performed with manual operations as described in Section 4.2.2. In such cases, semicontinuous multipass processing becomes identical to ordinary forming operations.

Greater interest and broader applications of semicontinuous ECAE of bulk billets for mass production at a metallurgical scale will require mechanization and automation of the handling operations. In our opinion, any future work must be focused toward this direction. As laid out here, the concept of an automated ECAE line is both realistic and practical. However, doing so may require substantial infrastructure investments and a thorough cost-benefit analysis of dimensional scaling of the ECAE tooling and rolling mill available for high-volume processing

of materials. However, if the project is awarded to proceed to Phase III and the search for an industrial partner(s) and necessary funding issues are resolved, EPM is capable of providing the required expertise, intellectual property, and technical leadership toward the successful realization of this new technology.

In conclusion, EPM greatly appreciates the US Army Small Business Administration, Army Research Laboratory, Ellwood Texas Forge Inc., and Manufacturing Science Corporation for their support and the opportunity to perform this project.

7. References

1. Hammond V, Jones T, Kecskes L, Mathaudhu S, Segal V. Fabrication of high-strength AA5083 for armor and structural applications through large-scale ECAE processing. Aberdeen Proving Ground (MD): Army Research Laboratory (US); 2014 Feb. Report No.: ARL-TR-6815.

2. Segal VM, Young PJ, Kecskes LJ. Fabrication of high-strength lightweight metals for armor and structural applications: large-scale equal channel angular extrusion processing of aluminum 5083 alloy. Aberdeen Proving Ground (MD): Army Research Laboratory (US); 2017 June. Report No.: ARL-TR-8047.

3. Jin H, Gallerneault M, Segal VM, Young PJ, Lloyd DJ. Grain structure and texture in aluminum alloy AA5083 after equal channel angular extrusion warm rolling and subsequent annealing. Mater Sci Technol. 2011;27:780–782.

4. Williams C, Sano T, Walter TR, Kecskes L. Microstructure effect of spall properties of 5083 aluminum: equal channel angular extrusion (ECAE) plus cold rolling. Proceedings of the 2016 Annual Conference on Experimental and Applied Mechanics; 2017. (Dynamic behavior of materials, Vol. 1.)

5. Vinogradov A, Serebryany VN, Dobatkin SV. Tailoring microstructure and properties of fine-grained magnesium alloys by severe plastic deformation-review. Adv Eng Mater. 2018;20:1700785.

6. Lenard J. Workability and process design in rolling. Handbook of workability and process design. In: Dieter E, Kuhn HA, Semiatin SL, editors. Novelty (OH): ASM International; 2003.

List of Symbols, Abbreviations, and Acronyms

AA	aluminum alloy
ARL	Army Research Laboratory
CCDC	US Army Combat Capabilities Development Command
DHS	die heating system
EBSD	electron backscatter diffraction
ECAE	equal channel angular extrusion
EPM	Engineered Performance Materials
EL	relative elongation
ETF	Ellwood Texas Forge
HRB	Rockwell hardness B scale
PLC	programmable logic controller
SBIR	Small Business Innovative Research
SC	semicontinuous
SEM	scanning electron microscopy
UTS	ultimate tensile strength
YS	yield stress

1 (PDF)	DEFENSE TECHNICAL INFORMATION CTR DTIC OCA
1 (PDF)	CCDC ARL FCDD RLD CL TECH LIB
1 (PDF)	GOVT PRINTG OFC A MALHOTRA
1 (PDF)	CCDC ARL FCDD RLW MF V HAMMOND